

Low-temperature specific-heat and neutron-diffraction studies on $\text{Li}_2\text{Pd}_3\text{B}$ and $\text{Li}_2\text{Pt}_3\text{B}$ superconductors

H. Takeya, K. Hirata, K. Yamaura, and K. Togano

National Institute for Materials Science, 1-2-1 Sengen, Tsukuba, Ibaraki 305-0047, Japan

M. El Massalami,* R. Rapp, and F. A. Chaves

Instituto de Física, Universidade Federal do Rio de Janeiro, Caixa Postal 68528, 21945-970 Rio de Janeiro, Brazil

B. Ouladdiaf

Institut Laue-Langevin, B.P. 156, 38042 Grenoble Cedex 9, France

(Received 9 May 2005; revised manuscript received 28 June 2005; published 9 September 2005)

Powder neutron diffraction analysis on ^{11}B -enriched samples of $\text{Li}_2\text{Pd}_3\text{B}$ and $\text{Li}_2\text{Pt}_3\text{B}$ confirms the stability, down to liquid helium temperatures, of their antiperovskite structure (space group $P4_332$). The low-temperature normal-state specific heats (measured within the range $400\text{ mK} < T < 20\text{ K}$ and $H \leq 70\text{ kOe}$) follow a superposition of a linear and a cubic term: for $\text{Li}_2\text{Pd}_3\text{B}$ the Sommerfeld coefficient $\gamma = 9.0(1)\text{ mJ/mol K}^2$ and the Debye temperature $\theta_D = 221(1)\text{ K}$ while for $\text{Li}_2\text{Pt}_3\text{B}$, $\gamma = 7.0(1)\text{ mJ/mol K}^2$ and $\theta_D = 228(1)\text{ K}$. Their thermodynamic superconducting temperatures T_c are, respectively, $7.5(3)\text{ K}$ and $2.17(5)\text{ K}$ while $\Delta C/\gamma T_c$ are $2.0(3)$ and $1.39(3)$. The thermal evolution of the superconducting specific heat of $\text{Li}_2\text{Pd}_3\text{B}$ is $C_{\text{es}}(T < T_c) = 22\gamma T_c \exp(-2.1T_c/T)\text{ J/mol K}$ while for $\text{Li}_2\text{Pt}_3\text{B}$ is $C_{\text{es}}(T < T_c) = 8.5\gamma T_c^2 \times \exp(-1.42T_c/T)\text{ J/mol K}$. The analysis of these features, within the framework of the strong-coupled theory, suggests that $\text{Li}_2\text{Pt}_3\text{B}$ is weakly coupled BCS-type superconductor [$T_c/\omega_{\text{log}} \rightarrow 0$, $\lambda = 0.48(2)$, $N(E_F) = 1.00(2)\text{ states/eV/formula unit}$, and $2\Delta_0/T_c = 3.53$] while $\text{Li}_2\text{Pd}_3\text{B}$ is an intermediate-coupled BCS-type superconductor [$T_c/\omega_{\text{log}} = 0.068(5)$, $\lambda = 1.09(7)$, $N(E_F) = 0.91(4)\text{ states/eV/formula unit}$, and $2\Delta_0/T_c = 3.94(4)$]. We discuss the reported reduction of T_c with x in the solid solution $\text{Li}_2(\text{Pt}_x\text{Pd}_{1-x})_3\text{B}$.

DOI: [10.1103/PhysRevB.72.104506](https://doi.org/10.1103/PhysRevB.72.104506)

PACS number(s): 74.70.Dd, 74.25.Ha, 74.62.Dh

I. INTRODUCTION

Recently superconductivity has been discovered in the antiperovskites $\text{Li}_2\text{Pd}_3\text{B}$ (Ref. 1) and $\text{Li}_2\text{Pt}_3\text{B}$ (Refs. 2 and 3). These compounds crystallize⁴ in the cubic space group $P4_332$, wherein the Pd/Pt atoms are arranged at the vertices of distorted octahedra that are centered by a B ion. The octahedra share all vertices and as such form an extended three-dimensional framework. Each of the Li atoms—situated in the space between the distorted octahedra—is surrounded by three Li nearest neighbors at a distance of 2.55 \AA ; such a Li-Li distance is less than that found in the Li metal (3.04 \AA), a feature considered by Eibenstein and Jung⁴ as indicative of electronic charge transfer from lithium to the Pd/B (Pt/B) network. It is not yet clear whether this charge transfer is the driving mechanism behind the surge of the superconductivity in these metal-rich borides; nonetheless, the presence of both a shorter Li-Li distance and a distorted octahedral remains a remarkable structural property, which deserves further studies. This work, utilizing the neutron powder diffraction analysis with its superior sensitivity for the lighter Li and B atoms, reports on the structural properties of these compounds with particular attention to their structural stability when the temperature is decreased down to the superconducting region.

The structural and normal-state properties of $\text{Li}_2\text{Pd}_3\text{B}$ and $\text{Li}_2\text{Pt}_3\text{B}$ are very similar. Both show similar metallic-type resistivity,^{2,3} with the same magnitude, the same thermal evolution, and the same ratio $\rho_{300\text{ K}}/\rho_{10\text{ K}} = 1.4$. In addition,

electronic structure calculations⁵ show that there is a similarity in the electron density distribution of both compounds, that the density of state at the Fermi level $N(E_F)$ is due predominantly to the d orbitals of the Pd/Pt atoms hybridized with B $2p$ and Li $2p$ states,⁶⁻⁸ and that the total $N(E_F)$ is larger in $\text{Li}_2\text{Pt}_3\text{B}$ than that in $\text{Li}_2\text{Pd}_3\text{B}$.

The superconducting parameters of $\text{Li}_2\text{Pd}_3\text{B}$ are substantially enhanced as compared to that of $\text{Li}_2\text{Pt}_3\text{B}$ (e.g., the superconducting transition point T_c of the former is three times higher than that of the latter).^{2,3,9} Such a tendency is clearly manifested in the systematic studies on the solid solution $\text{Li}_2(\text{Pt}_x\text{Pd}_{1-x})_3\text{B}$:^{2,3} as a matter of fact, T_c varies almost linearly with x . Considering the remarkable similarity between their structural and normal-state electronic properties and, furthermore, that there are no obvious pair-breaking mechanism(s), it is then surprising that their superconducting properties, in particular T_c , are much different. It is then of interest to investigate the cause of such a variation and as well the pairing mechanism in these metal-rich ternary borides and therefrom deduce the origin of the almost linear behavior of T_c with x . As a contribution in that direction, it is most appropriate to undertake specific heat measurements so as to probe the low-temperature thermal and electronic properties of the two end members of this series. Then it is possible to judge whether there is any correlation between the superconductivity, the thermal/electronic properties, and the content of the Pt/Pd atoms. With that objective in mind, in this work we report on the specific-heat measurements on $\text{Li}_2\text{Pd}_3\text{B}$ and

$\text{Li}_2\text{Pt}_3\text{B}$ within the range $0.4 \text{ K} < T < 20 \text{ K}$ and in a magnetic field up to 70 kOe (a limit that is higher than H_{c2}).

II. EXPERIMENTAL

Samples were prepared by a two-stage arc-melting process (for details, see Ref. 1). Basic characterizations such as room-temperature x-ray diffraction, magnetization, and resistivity were carried out, and the obtained results are in good agreement with the published data.²⁻⁴ This is particularly valid for the XRD results, however, since the x-ray diffractometry is less sensitive to the lighter elements, we also carried out powder neutron diffraction analysis on ^{11}B -enriched samples. These measurements were carried out between 2 and 300 K at the Institut Laue-Langevin in Grenoble, France; patterns of $\text{Li}_2\text{Pt}_3\text{B}$ were collected using the D1A diffractometer with a selected $\lambda = 1.91 \text{ \AA}$ while for those of $\text{Li}_2\text{Pd}_3\text{B}$, the D2B diffractometer was used with $\lambda = 1.595 \text{ \AA}$. Rietveld refinements were carried out using the FULLPROF package of Rodriguez-Carvajal (L. L. B.).

The specific heat measurements were carried out on two different types of calorimeters. A zero-field semiadiabatic calorimeter operated within the range $400 \text{ mK} < T < 20 \text{ K}$ and having a precision of better than 4%. The other is a relaxation-type calorimeter (a commercial one from Quantum Design) that was operated within the range $2 \text{ K} < T < 20 \text{ K}$ and $H \leq 70 \text{ kOe}$.

III. RESULTS AND ANALYSIS

A. Neutron powder diffraction

The low-temperature diffractograms of both compounds are shown in Fig. 1. The results of the refinements (see Table I) confirm the room-temperature structural model of Eibenstein and Jung⁴ within our statistics and considering the temperature difference, all the parameters (specifically position, occupation, and anisotropic thermal parameters) are almost equal to the reported ones.⁴ For the particular case of $\text{Li}_2\text{Pt}_3\text{B}$, the a parameter is $6.7465(1) \text{ \AA}$ at 300 K while $6.7345(1) \text{ \AA}$ at 2 K: only a 0.18% difference that is due to thermal contraction. It is worth recalling that, due to the Li nonstoichiometry, there is some minor variation among the lattice parameters of different patches of the same compound, even when measured at the same temperature.

The position parameters of Li and Pt/Pd atoms that are not fixed by symmetry are very similar to those of Eibenstein and Jung⁴ (see Table I) and, in addition, they do not show any noticeable variation on going from 300 down to 2 K. Based on these and the above-mentioned findings, it is inferred that the basic room-temperature structural features remains unaltered. Specifically, the Li-Li distance is hardly modified on lowering the temperature; as a consequence the charge transfer to the T/B network, if solely governed by Li-Li distance, is unaffected by such temperature variations.

B. Specific heat

The specific heat of $\text{Li}_2\text{Pd}_3\text{B}$ is shown in Fig. 2. Its normal state properties were achieved after quenching the super-

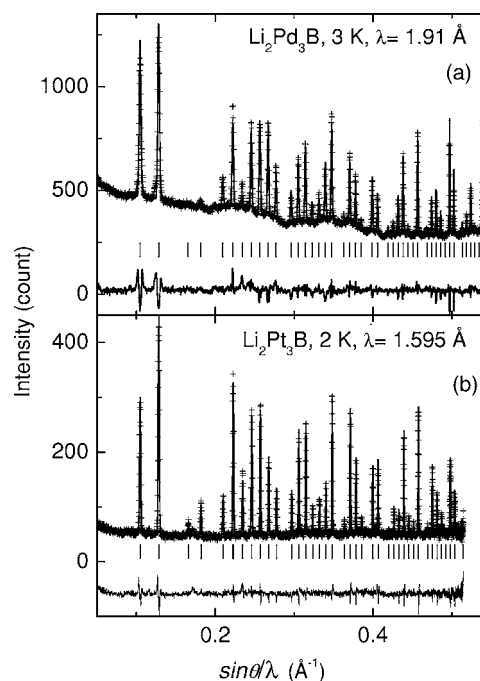


FIG. 1. Neutron powder diffractograms of (a) $\text{Li}_2\text{Pd}_3\text{B}$ at 3 K and (b) $\text{Li}_2\text{Pt}_3\text{B}$ at 2 K. For each panel, symbols represent the total measured diffraction intensity while the solid line gives the calculated pattern. The difference curve is shown at the bottom while the Bragg positions are indicated as short bars. Some refined parameters are given in Table I. The reliability factors for $\text{Li}_2\text{Pt}_3\text{B}$ (having, relatively, better statistics) are $R_B = 5.5$ and $R_F = 3.9$.

conductivity in a magnetic field of 70 kOe ($> H_{c2}$).¹ Under such a condition, the normal-state specific heat is adequately described by a superposition of a Sommerfeld (γT) and Debye (βT^3) term: in a region of $2 \text{ K} < T < 5 \text{ K}$, the normal-state coefficients are $\gamma = 9.0(1) \text{ mJ/mol K}^2$ and $\beta = 1.08(1) \text{ mJ/mol K}^4$.

The zero-field specific heat of $\text{Li}_2\text{Pt}_3\text{B}$ is shown in Fig. 3. Its normal-state specific heat was analyzed as a sum of a linear and a cubic term; here also the analysis had been limited to the range $T_c < T < 5 \text{ K}$. The fit is excellent, giving $\gamma = 7.0(1) \text{ mJ/mol K}^2$ and $\beta = 0.98(1) \text{ mJ/mol K}^4$. Assuming no (drastic) modification in the normal-state properties due to the 70 kOe field, a comparison of γ and β of the two compounds (see Table II) suggests that for the case of $\text{Li}_2\text{Pd}_3\text{B}$, γ is almost 30% higher while the Debye temperature, θ_D , is only 3% lower; evidently only the difference between their γ is significant. Such an enhancement of γ could be due to an increase in the single-spin electron density of state at the Fermi level $N(E_F)$ or in the electronic mass-enhancement parameter λ :

$$\gamma = \frac{2}{3} \pi^2 k_B^2 (1 + \lambda) N(E_F). \quad (1)$$

As λ appears also in expressions governing the superconducting properties of these compounds (see below), then it is possible to evaluate separately each of $N(E_F)$ and λ ; in an-

TABLE I. Structural parameters of $\text{Li}_2\text{Pd}_3\text{B}$ and $\text{Li}_2\text{Pt}_3\text{B}$, as measured by powder room-temperature x-ray diffraction (Ref. 4) and low-temperature powder neutron diffraction (this work). a is the cubic unit-cell parameter, x_T is the parameter appearing in the relative position of Pd/Pt ($1/8, x_T, 1/4 - x_T$) having Wyckoff notation $12d$. Similarly x_{Li} represents the position of Li ($x_{\text{Li}}, x_{\text{Li}}, x_{\text{Li}}$) with Wyckoff notation $8c$. Due to Li nonstoichiometry, care should be exercised on comparing structural parameters of different preparation of the same compounds (see the text).

$\text{Li}_2\text{T}_3\text{B}$	X-ray diffraction ⁴				Neutron diffraction (this work)			
	T[K]	$a[\text{\AA}]$	x_T	x_{Li}	T[K]	$a[\text{\AA}]$	x_T	x_{Li}
Pd	300	6.7534(3)	0.30417(5)	0.3072(9)	3	6.7485(2)	0.3052(2)	0.3037(5)
Pt	300	6.7552(5)	0.3079(2)	0.293(7)	2	6.7345(1)	0.3087(1)	0.3031(1)

ticipation, the enhancement of γ is due mainly to an increase in λ (see below).

From the analysis of the specific heats at the onset of the superconducting state (Figs. 2 and 3) and utilizing the balance of entropy (see the inset of Fig. 3), we extracted the values of T_c and $\Delta C/\gamma T_c$ (the specific-heat jump at T_c): T_c of $\text{Li}_2\text{Pd}_3\text{B}$ is 7.5(2) K while that of $\text{Li}_2\text{Pt}_3\text{B}$ is 2.17(5) K (both agree very well with the reported values^{1,3}). $\Delta C/\gamma T_c$ is 2.0(3) for $\text{Li}_2\text{Pd}_3\text{B}$ while 1.39(3) for $\text{Li}_2\text{Pt}_3\text{B}$: since for a standard BCS superconductor $\Delta C/\gamma T_c = 1.43$, it is evident that $\text{Li}_2\text{Pt}_3\text{B}$ agrees quite reasonably with the weakly-coupled BCS prediction, but $\text{Li}_2\text{Pd}_3\text{B}$ deviates appreciably due to strong-coupling effects (see below). It is worth mentioning that for the particular case of $\text{Li}_2\text{Pd}_3\text{B}$, the large errors in $\Delta C/\gamma T_c$ and T_c are due to an almost-1 K-broadened-transition region, which, according to Togano *et al.*,¹ is due to the nonstoichiometry of lithium. For this reason, we did not evaluate the thermal evolution of $\Delta C(T)/\gamma T$ in the neighborhood of T_c nor its thermal derivative at T_c .

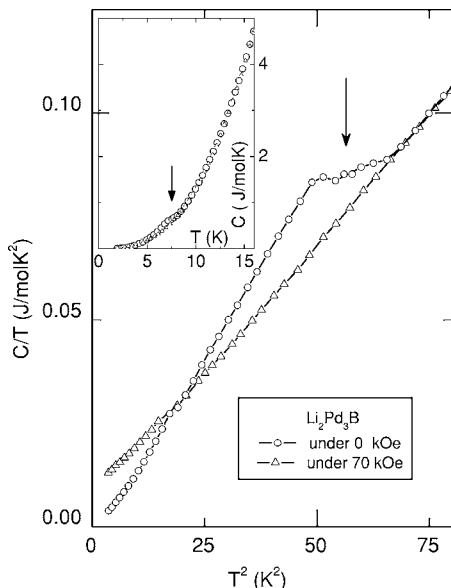


FIG. 2. The C/T vs T^2 curve of the superconducting (circle) and normal (triangle) phases of $\text{Li}_2\text{Pd}_3\text{B}$. Here C represents the total specific heat (lines are a guide to the eye). Inset: the C vs T curve over an extended temperature range. The arrows indicate the superconducting transition temperature as obtained from the balance of entropies.

The analysis of the electronic specific heat within the superconducting phase $C_{\text{es}}(T)$ of $\text{Li}_2\text{Pd}_3\text{B}$ is shown in Fig. 4 while that of $\text{Li}_2\text{Pt}_3\text{B}$ in Fig. 5. Evidently in both figures, $C_{\text{es}}(T)$ reflects clearly an exponential behavior, indicative of a gap character. For $\text{Li}_2\text{Pd}_3\text{B}$, the solid line represents $C_{\text{es}}(T) = 22\gamma T_c \exp(-2.1T_c/T)$ J/mol K while for $\text{Li}_2\text{Pt}_3\text{B}$, $C_{\text{es}}(T) = 8.5\gamma T_c \exp(-1.42T_c/T)$ J/mol K. It is recalled that for a weak-coupled BCS superconductor,¹⁰ $C_{\text{es}}(T) = 8.5\gamma T_c \exp(-1.44T_c/T)$ for $2.5 < T_c/T < 6$, $C_{\text{es}}(T) = 26\gamma T_c \exp(-1.62T_c/T)$ for $7 < T_c/T < 12$, and $C_{\text{es}}(T) = 3.15\gamma T_c(T_c/T)^{1.5} \exp(-1.76T_c/T)$ for $T \rightarrow 0$. On comparing these equations with the experimental curves, it is inferred that $C_{\text{es}}(T)$ of $\text{Li}_2\text{Pt}_3\text{B}$ follows reasonably well the prediction of the BCS model: the small upward deviation at a lower temperature is assumed to be due to contributions from extrinsic effects such as impurities or nonstoichiometry. On the other hand, $C_{\text{es}}(T)$ of $\text{Li}_2\text{Pd}_3\text{B}$ does follow the exponential behavior, but with factors that are differing from those predicted by the above-mentioned BCS equations: this deviation

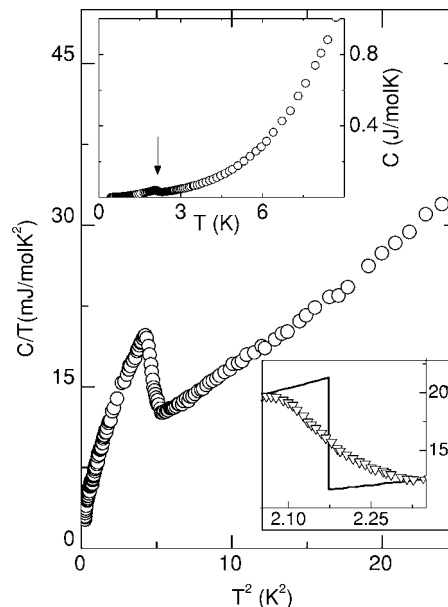


FIG. 3. The C/T vs T^2 plot of $\text{Li}_2\text{Pt}_3\text{B}$. Upper inset: the total specific heat versus temperature. Lower inset: the equal-area construction wherein the experimental (triangles) and extrapolated (solid line) C/T are plotted against the temperature; the vertical axis of the lower inset is in mJ/mol K^2 while the horizontal one is in K.

TABLE II. Normal and superconducting parameters of $\text{Li}_2\text{Pd}_3\text{B}$ and $\text{Li}_2\text{Pt}_3\text{B}$. All terms have their usual definitions. (Renormalized) BCS relations [Eq. (2)] are used for the calculation on $\text{Li}_2\text{Pt}_3\text{B}$, while their corresponding strong-coupling corrections [Eqs. (3)–(5)] are used for the calculation on $\text{Li}_2\text{Pd}_3\text{B}$. Standard deviations are included for the calculated quantities. Note that the pre-exponential factor in Eq. (2) is $\theta_D/1.45$ while that in Eq. (5) is $\omega_{\text{in}}/1.2$ (Ref. 13). For $\text{Li}_2\text{Pt}_3\text{B}$, if instead of θ_D we use $\omega_{\text{in}} \approx \omega_{\text{in}}(\text{Li}_2\text{Pd}_3\text{B}) = 110$ K, then λ is increased by 13% while $N(E_F)$ is decreased by 4%. Thus, on a simple comparison, all conclusions reached in this work still hold.

$\text{Li}_2\text{T}_3\text{B}$	Experiment				Calculation					
	T_c K	γ mJ/mol K ²	θ_D K	$\Delta C/\gamma T_c$	ω_{in} K	T_c/ω_{in}	$2\Delta_0/T_c$	$2\Delta_0$ K	λ	$N(E_F)$ 1/eV/fu
$\text{Li}_2\text{Pd}_3\text{B}$	7.5(3)	9.0(1)	221(1)	2.0(3)	110(10)	0.068(5)	3.94(4)	29.6(1.0)	1.09(7)	0.91(4)
$\text{Li}_2\text{Pt}_3\text{B}$	2.17(5)	7.0(1)	228(1)	1.39(3)	-	≈ 0	3.53	7.7(2)	0.48(2)	1.00(2)

is considered to be due to strong-coupling corrections.

Finally, the ratio $\theta_{D,\text{Pt}}\sqrt{M_{\text{Pt}}}/(\theta_{D,\text{Pd}}\sqrt{M_{\text{Pd}}}) \approx 1.4$ is 40% higher than expected. Similarly, the partial isotope relation $T_{c,\text{Pt}}\sqrt{M_{\text{Pt}}}/T_{c,\text{Pd}}\sqrt{M_{\text{Pd}}} \approx 0.4$ is 60% away from the prediction of the standard BCS model. The difficulty in controlling the Li stoichiometry discouraged us from studying the isotope effect in these superconductors: it was reported earlier¹ that T_c strongly depends on the stoichiometry of the Li atom, reminiscent of the carbon nonstoichiometry in the similar antiperovskite MgCNi_3 .¹¹ A similar Li dependence of T_c is expected to be present in the $\text{Li}_2(\text{Pt}_x\text{Pd}_{1-x})_3\text{B}$ series,^{2,3} however, such a nonstoichiometry cannot account for the linear decrease of T_c with x .

IV. DISCUSSION AND CONCLUSION

According to the above-shown specific heats, the low-temperature normal-state electronic and thermal properties of the studied compounds can be described, respectively, within the Sommerfeld and Debye approximations. The range of γ

indicates a conventional Fermi liquid behavior. Further, the bulk character of their superconductivities is clearly revealed and that the evolution of their specific heat within the superconducting phase is indicative of a thermal activation across a superconducting gap: for $\text{Li}_2\text{Pd}_3\text{B}$ the conventional gapped superconductivity is in line with the findings of Nishiyama *et al.*⁷ On checking this exponential character and the ranges of $\Delta C/\gamma T_c$ against the predictions of the renormalized BCS model, it is concluded that $\text{Li}_2\text{Pt}_3\text{B}$ is a weak-coupled BCS superconductor with, presumably, an electron-phonon pairing mechanism. The characteristic (superconducting) parameters of $\text{Li}_2\text{Pt}_3\text{B}$ (see Table II) were evaluated based on the BCS-type relations, namely^{12–14}

$$[\Delta C/\gamma T_c]_{T_c} = 1.43, \quad 2\Delta_0/k_B T_c = 3.53, \quad \text{and}$$

$$T_c = (\theta_D/1.45)\exp[-(1+\lambda)/(\lambda-\mu^*)], \quad (2)$$

where $2\Delta_0$ is the superconductivity gap at zero temperature and μ^* is the Coulomb pseudopotential, which, according to

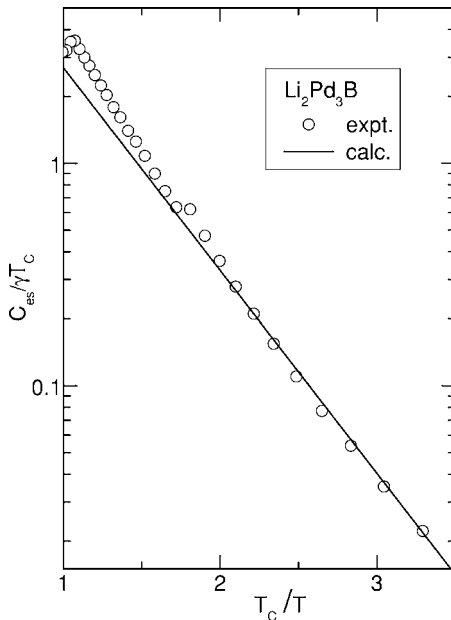


FIG. 4. Reduced electronic specific heat $C_{\text{es}}/\gamma T_c$ vs reduced temperature T_c/T of $\text{Li}_2\text{Pd}_3\text{B}$. The solid lines indicates the calculated, normalized specific heat: $C_{\text{es}}(T)/\gamma T_c = 22 \exp(-2.1T_c/T)$.

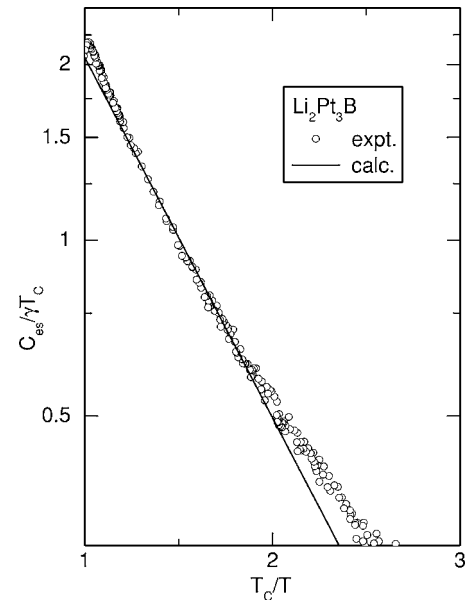


FIG. 5. Reduced electronic specific heat $C_{\text{es}}/\gamma T_c$ vs reduced temperature T_c/T of $\text{Li}_2\text{Pt}_3\text{B}$. The solid lines indicates the calculated, normalized specific heat: $C_{\text{es}}(T)/\gamma T_c = 8.5 \exp(-1.42T_c/T)$. The low-temperature deviation is discussed in the text.

Chandara *et al.*,⁵ can be significant in these compounds (taken here to be 0.13).

The above quoted weak-coupling relations are found to be inadequate for the case of $\text{Li}_2\text{Pd}_3\text{B}$. Considering the structural and electronic isomorphism between these two compounds, the superconductivity of $\text{Li}_2\text{Pd}_3\text{B}$ is considered to be of the same character as that of $\text{Li}_2\text{Pt}_3\text{B}$ —the assumption of phonon mediation is in line with the arguments Refs. 6 and 7—but with a relatively stronger coupling constant. Indeed, its measured superconducting properties compare favorably with the following strong-coupling corrections (valid for $T_c/\omega_{\log} \ll 1$):¹²⁻¹⁴

$$[\Delta C/\gamma T_c]_{T_c} = 1.43[1 + 53(T_c/\omega_{\log})^2 \ln(\omega_{\log}/3T_c)], \quad (3)$$

$$2\Delta_0/k_B T_c = 3.53[1 + 12.5(T_c/\omega_{\log})^2 \ln(\omega_{\log}/2T_c)], \quad (4)$$

$$T_c = \frac{\omega_{\log}}{1.2} \exp\left(-\frac{1.04(1 + \lambda)}{\lambda - \mu^*(1 + 0.62\lambda)}\right), \quad (5)$$

where ω_{\log} is a characteristic phonon temperature defined as the logarithmic moment of the electron-phonon spectral function $\alpha^2 F(\omega)$. The various constants were extracted by the usual procedure (see, e.g., Ref. 15): first, based on Eq. (3) and using the experimentally measured $\Delta C/\gamma T_c$, we determined ω_{\log} and, thereafter, $2\Delta_0$ [Eq. (4)] and λ [Eq. (5)]. Finally, based on Eq. (1) together with γ and λ , $N(E_F)$ was evaluated.

In light of the calculated results of $\text{Li}_2\text{Pd}_3\text{B}$ (see Table II), it is evident that the condition $T_c/\omega_{\log} \ll 1$ is reasonably satisfied and, moreover, the range of the calculated parameters does emphasize its intermediate-coupled character, particularly when compared with the weak-coupled character of $\text{Li}_2\text{Pt}_3\text{B}$. Its λ is 1.09(7) while that of the Pt-based isomorph is 0.480(2): a factor-of-2 enhancement. Furthermore, its $N(E_F)$ is 0.91(4) states/(eV-formula unit) while that of $\text{Li}_2\text{Pt}_3\text{B}$ is 1.00(2) states/(eV-formula unit): a decreasing trend that is opposite to the one manifested for λ , T_c , and γ . This trend is evident also in the electronic structure calculation:⁵ for $\text{Li}_2\text{Pd}_3\text{B}$, $N(E_F)_{\text{cal}} \approx 1.3$ states/(eV-formula unit) while for $\text{Li}_2\text{Pt}_3\text{B}$, $N(E_F)_{\text{cal}} \approx 1.5$ states/(eV-formula unit); remarkably, both are within a 30%–50% difference from the experimentally determined ones. It is worth noting that such an increase in $N(E_F)$ is certainly not determined solely by the Li-Li distance, otherwise an increase in the Pt content (leading to an increase in the Li-Li distance) should induce, according to Eibenstein and Jung, a decrease in the amount of the would-be-transferred Li-electrons.

Evidently, both experiment and theory⁵ indicate that $N(E_F)$ of $\text{Li}_2\text{Pd}_3\text{B}$ is a $\sim 10\%$ lower than that of $\text{Li}_2\text{Pt}_3\text{B}$. That λ and T_c of $\text{Li}_2\text{Pd}_3\text{B}$ are higher even though its $N(E_F)$ is lower can be understood within the framework of the strong-coupled theory:¹²⁻¹⁴

$$\lambda = N(E_F)\langle I^2 \rangle / M\langle \omega^2 \rangle = \eta / M\langle \omega^2 \rangle, \quad (6)$$

where M is the atomic mass, $\langle \omega^2 \rangle$ is an average over the Fermi surface of the squared phonon frequency, and $\langle I^2 \rangle$ is an average of the squared electron-phonon matrix element. $\eta = N(E_F)\langle I^2 \rangle$ is a purely electronic property, which, according to McMillan,¹² remains constant within the same class of materials and, as such, λ would be dictated principally by the phonon factor $M\langle \omega^2 \rangle$. For checking the validity of this statement in the particular case of ternary borides, a knowledge of η and $\langle \omega^2 \rangle$ is necessary; in that respect, the Debye temperature is not a sufficiently reliable estimate of $\langle \omega^2 \rangle$.¹²⁻¹⁴ Rather, $\alpha^2 F(\omega)$, when available, would provide information on how $\langle \omega^2 \rangle$ (as well as λ and ω_{\log}) varies. Here, for want of a better criterion, we use the experimental finding that the product λM (where M is the atomic mass of Pt or Pd) is roughly the same: for $\text{Li}_2\text{Pt}_3\text{B}$, $\lambda M = 94$ while for $\text{Li}_2\text{Pd}_3\text{B}$ $\lambda M = 106$. Then Eq. (6) demands that the factors $\eta/\langle \omega^2 \rangle$ of both compounds should be equal. Since $N(E_F)$ of the Pd-based compound is lower, its factor $\langle I^2 \rangle/\langle \omega^2 \rangle$ must be higher, and this may be brought about by (i) an increase in $\langle I^2 \rangle$: a relatively small-sized Pd atom permits a stronger contraction of the d wave functions toward the core; as a consequence, the electron-phonon matrix element increases,¹³ or (ii) a softening in $\langle \omega^2 \rangle$. Whatever may be the case, it is evident that the increase in the factor $\langle I^2 \rangle/\langle \omega^2 \rangle$ [sufficient enough to overcome the decrease in $N(E_F)$] is the driving mechanism behind the enhancement of the superconductivity in $\text{Li}_2\text{Pd}_3\text{B}$ as compared to $\text{Li}_2\text{Pt}_3\text{B}$. This mechanism is expected to be operative as well in the intermediate alloys of the $\text{Li}_2(\text{Pt}_x\text{Pd}_{1-x})_3\text{B}$ series. In fact, Eq. (5) does suggest a monotonic, smooth, and apparently linear variation of T_c with x , assuming no variation in the superconducting character and that the parameters such as $N(E_F)$, $\langle I^2 \rangle$, and $\langle \omega^2 \rangle$ vary reasonably with x .

ACKNOWLEDGMENTS

We acknowledge the partial financial support from the Japan Society for the Promotion of Science and the Brazilian agencies CNPq and Faperj.

*Corresponding author.

¹K. Togano, P. Badica, Y. Nakamori, S. Orimo, H. Takeya, and K. Hirata, *Phys. Rev. Lett.* **93**, 247004 (2004).

²P. Badica, T. Kondo, and K. Togano, *J. Phys. Soc. Jpn.* **74**, 1014 (2005).

³P. Badica, T. Kondo, T. Kudo, Y. Nakamori, S. Orimo, and K.

Togano, *Appl. Phys. Lett.* **85**, 4433 (2004).

⁴U. Eibenstein and W. Jung, *J. Solid State Chem.* **133**, 21 (1997).

⁵S. Chandra, S. N. Jaya, and M. C. Valsakumar, *cond-mat/0502525*, 2005.

⁶T. Yokoya, T. Muro, I. Hase, H. Takeya, K. Hirata, and K. Togano, *Phys. Rev. B* **71**, 092507 (2005).

- ⁷M. Nishiyama, Y. Inada, and G. Q. Zheng, *Phys. Rev. B* **71**, 220505(R) (2005).
- ⁸M. Sardar and D. Sa, *Physica C* **411**, 120 (2004).
- ⁹H. Q. Yuan, D. Vandervelde, M. B. Salamon, P. Badica, and K. Togano, cond-mat/0506771, 2005.
- ¹⁰E. S. R. Gopal, *Specific Heat at Low Temperatures* (Plenum, New York, 1966).
- ¹¹T. He, Q. Huang, A. P. Ramirez, Y. Wang, K. A. Regan, N. Rogado, M. A. Hayward, M. K. Haas, J. S. Slusky, K. Inumara H. W. Zandbergen, N. P. Ong, R. J. Cava, *Nature (London)* **411**, 54 (2001).
- ¹²W. L. McMillan, *Phys. Rev.* **167**, 331 (1968).
- ¹³P. B. Allen and R. C. Dynes, *Phys. Rev. B* **12**, 905 (1975).
- ¹⁴J. P. Carbotte, *Rev. Mod. Phys.* **62**, 1027 (1990).
- ¹⁵M. Ishikawa and E. Toth, *Phys. Rev. B* **3**, 1856 (1971).